Toxicology and Applied Pharmacology 272 (2013) 117–126

Contents lists available at ScienceDirect

Toxicology and Applied Pharmacology

journal homepage: www.elsevier.com/locate/ytaap

# (4-Methoxyphenyl)(3,4,5-trimethoxyphenyl)methanone inhibits tubulin polymerization, induces $G_2$/M arrest, and triggers apoptosis in human leukemia HL-60 cells

Hemerson I.F. Magalhães [a,d], Diego V. Wilke [a], Daniel P. Bezerra [b,*], Bruno C. Cavalcanti [a], Rodrigo Rotta [c], Dênis P. de Lima [c], Adilson Beatriz [c], Manoel O. Moraes [a], Jairo Diniz-Filho [a], Claudia Pessoa [a,*]

[a] Departamento de Fisiologia e Farmacologia, Faculdade de Medicina, Universidade Federal do Ceará, Fortaleza, Ceará, Brazil
[b] Centro de Pesquisa Gonçalo Moniz, Fundação Oswaldo Cruz, Salvador, Bahia, Brazil
[c] Centro de Ciências Exatas e Tecnológicas (Laboratório LP4), Universidade Federal do Mato Grosso do Sul, Campo Grande, Mato Grosso do Sul, Brazil
[d] Centro de Ciências da Saúde, Departamento de Ciências Farmacêuticas, Universidade Federal da Paraíba, João Pessoa, Paraíba, Brazil

ARTICLE INFO

*Article history:*
Received 6 April 2013
Revised 16 May 2013
Accepted 2 June 2013
Available online 10 June 2013

*Keywords:*
Phenstatins
Tubulin inhibitors
Apoptosis
Caspase activation

ABSTRACT

(4-Methoxyphenyl)(3,4,5-trimethoxyphenyl)methanone (PHT) is a known cytotoxic compound belonging to the phenstatin family. However, the exact mechanism of action of PHT-induced cell death remains to be determined. The aim of this study was to investigate the mechanisms underlying PHT-induced cytotoxicity. We found that PHT displayed potent cytotoxicity in different tumor cell lines, showing $IC_{50}$ values in the nanomolar range. Cell cycle arrest in $G_2$/M phase along with the augmented metaphase cells was found. Cells treated with PHT also showed typical hallmarks of apoptosis such as cell shrinkage, chromatin condensation, phosphatidylserine exposure, increase of the caspase 3/7 and 8 activation, loss of mitochondrial membrane potential, and internucleosomal DNA fragmentation without affecting membrane integrity. Studies conducted with isolated tubulin and docking models confirmed that PHT binds to the colchicine site and interferes in the polymerization of microtubules. These results demonstrated that PHT inhibits tubulin polymerization, arrests cancer cells in $G_2$/M phase of the cell cycle, and induces their apoptosis, exhibiting promising anticancer therapeutic potential.



## Introduction

Tubulins are the proteins that make up microtubules. The microtubules are important for diverse cellular functions, including chromosome segregation during cell division, intracellular transport, and cell motility. Drugs that interact with tubulin interfere in microtubule dynamics, altering their functionality and producing fatal consequences on cells under division processes. Once those cancer cells show high mitotic rates, tubulins are targets for anticancer drugs (Dumontet and Jordan, 2010; Jordan and Kamath, 2007). There are three well-characterized sites for ligands in tubulin: taxanes, vinca alkaloids, and colchicine sites. These agents either inhibit the polymerization of tubulin (vinca alkaloids and colchicine) or prevent the microtubule disassembly (taxanes) (Buey et al., 2005; Dumontet and Jordan, 2010; Jordan and Kamath, 2007; Lobert et al., 1999).

There are several drugs reported that target the colchicine binding site and some of these are currently in clinical trials as anticancer agents, including combretastatin A-4 (CA-4). Phenstatin is a CA-4 analog which the double bond is replaced by a carbonyl group (Cushman et al., 1992; Liou et al., 2002, 2004; Pettit et al., 1998). Phenstatin and related compounds display high potencies in both inhibition of tubulin polymerization and cytotoxicity against tumor cell lines (Alvarez et al., 2008, 2009, 2010; Pettit et al., 1998).

(4-Methoxyphenyl)(3,4,5-trimethoxyphenyl)methanone (PHT, Fig. 1) is a known cytotoxic compound belonging to the phenstatin family. This compound has been studied because of its potent cytotoxicity and antitubulin properties (Alvarez et al., 2009; Barbosa et al., 2009; Liou et al., 2002). Magalhães et al. (2011a) showed that PHT also displays *in vivo* antitumor effects, without substantial side effects. Additionally, PHT also was able to induce DNA damage and clastogenic effects in human lymphocytes (Magalhães et al., 2011b). However, the exact mechanism of action of PHT-induced cell death remains to be determined. In this study, we investigated the mechanisms underlying PHT-induced cytotoxicity.

*Abbreviations:* BrdU, 5-bromo-20-deoxyuridine; CA-4, combretastatin A-4; CA-4P, combretastatin-A4-phosphate; DI, damage index; MTT, 3-(4,5-dimethyl-2-thiazolyl)-2,5-diphenyl-2H-tetrazolium bromide; PHT, (4-methoxyphenyl)(3,4,5-trimethoxyphenyl) methanone; TNF-α, tumor necrosis factor-α; ROS, reactive oxygen species.

* Corresponding authors. Fax: +55 85 3366 8333.
*E-mail addresses:* danielpbezerra@gmail.com (D.P. Bezerra), c_pessoa@yahoo.com (C. Pessoa).

0041-008X/$ – see front matter © 2013 Elsevier Inc. All rights reserved.
http://dx.doi.org/10.1016/j.taap.2013.06.001

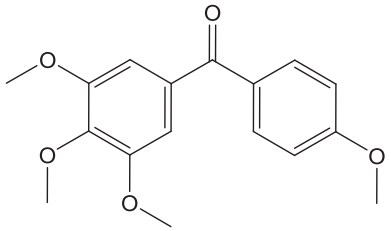

**Fig. 1.** Chemical structure of (4-methoxyphenyl)(3,4,5-trimethoxyphenyl)methanone (PHT).

## Material and methods

*(4-Methoxyphenyl)(3,4,5-trimethoxyphenyl)methanone (PHT) synthesis.* The preparation of PHT was performed as previously described (Alvarez et al., 2009; Barbosa et al., 2009; Magalhães et al., 2011a). The reaction was carried out in a one-neck, 250 ml round-bottomed flask fitted with a condenser with drying tube. Anhydrous dichloromethane (20 ml), 3,4,5-trimethoxybenzoic acid (1.4 g, 6.6 mmol), and thionyl chloride (1.57 g, 13.2 mmol) were added to the flask. The mixture was refluxed for 4 h and, after cooling to room temperature, the solvent was removed with a rotary evaporator. Dichloromethane (25 ml) was added to the flask and cooled to 0 °C. With good stirring, anhydrous aluminum chloride (0.44 g, 3.3 mmol) and anisole (0.72 g, 6.6 mmol) were slowly added into the reaction vessel during 10 min. After the addition, the reaction mixture was stirred at room temperature for 30 min and then ice-cold hydrochloric acid (20 ml) was poured into the flask. The product was extracted with dichloromethane and washed with cold sodium bicarbonate solution and water. The organic layer was dried with $MgSO_4$ and, after filtration; the solvent was removed using a rotary evaporator. The residue was purified by flash chromatography using an eluent of 5:1 hexane:ethyl acetate. A colorless crystalline solid was obtained. ES/MS: 303.2026 [M + 1], yield = 80%, m.p. = 67–68 °C.

*Cell lines and cell culture.* The cytotoxicity of PHT was tested against HL-60 (human leukemia), B-16 (murine melanoma), B-16-F10 (murine melanoma), CEM (human leukemia), K-562 (human leukemia), Jurkat (human leukemia), MDA-MB-231 (human breast carcinoma), MX-1 (human breast carcinoma), and PC-3 (human prostate carcinoma) cancer cell lines, all of them donated by the National Cancer Institute, Bethesda, MD, USA. Cells were grown in RPMI-1640 medium supplemented with 10% fetal bovine serum, 2 mM glutamine, 100 μg/ml streptomycin, and 100 U/ml penicillin, and incubated at 37 °C in a 5% $CO_2$ atmosphere.

*MTT assay.* Tumor cell growth was determined by the ability of living cells to reduce the yellow dye 3-(4,5-dimethyl-2-thiazolyl)-2,5-diphenyl-*2H*-tetrazolium bromide (MTT, Sigma Chemical Co. St Louis, MO, USA) to a purple formazan product (Mosmann, 1983). For all experiments, 100 μl of cells was seeded in 96-well plates ($0.7 \times 10^5$ cells/ml for adherent cells or $0.3 \times 10^6$ cells/ml for suspended cells). After 24 h, PHT (0.009–5 μg/ml) was added to each well (using the HTS — high-throughput screening — Biomek 3000; Beckman Coulter Inc., Fullerton, CA, USA) and the cells were incubated for 72 h. Doxorubicin (Sigma Chemical Co. St Louis, MO, USA) was used as the positive control. At the end of incubation, the plates were centrifuged and the medium was replaced by fresh medium (150 μl) containing 0.5 mg/ml MTT. Three hours later, the formazan product was dissolved in 150 μl DMSO and the absorbance was measured using a multiplate reader (DTX 880 Multimode Detector, Beckman Coulter Inc., Fullerton, CA, USA). The drug effect was expressed as the percentage of control absorbance of reduced dye at 595 nm.

*Cell viability curve.* Cell viability was determined by the trypan blue dye exclusion test. HL-60 cells were seeded ($0.3 \times 10^6$ cells/ml) in the absence or presence of different concentrations of PHT (0.25, 0.5, 1.0, 2.0, and 4.0 μM). After each incubation period (3, 6, 12, 18, and 24 h), a growth curve was established. Cells that excluded trypan blue were counted using a Neubauer chamber (LO, Laboroptik GmbH, Bad Homburg, Hessen, Germany).

The following experiments were performed in order to elucidate the mechanisms involved in PHT cytotoxic action on HL-60 cells after 24 h incubation. The trypan blue exclusion test was also performed before each experiment described below to assess cell viability. Negative control was treated with the vehicle (0.1% DMSO) used for diluting the tested substance. Doxorubicin (0.5 μM) was used as the positive control. Doxorubicin, clinically useful chemotherapeutic agent, was used as the positive control due its high cytotoxicity and wide use to induce apoptosis with high reproducibility of the results.

*BrdU incorporation assay.* Twenty microliters of 5-bromo-20-deoxyuridine (BrdU, 10 mM) was added to each well and incubated for 3 h at 37 °C before completing the 24 h period of drug exposure. To access the amount of BrdU incorporated into DNA, cells were harvested, transferred to cytospin slides (Shandon Southern Products Ltd., Sewickley Pennsylvania, USA), and allowed to dry for 2 h at room temperature. Cells that had incorporated BrdU were labeled by direct peroxidase immunocytochemistry using the chromogen diaminobenzidine. Slides were counterstained with hematoxylin, mounted, and coverslipped. Evaluation of BrdU-positivity was made by light microscopy (Olympus, Tokyo, Japan). Two hundred cells were counted per sample to determine the percentage of positive cells.

*Morphological analysis with hematoxylin–eosin staining.* Untreated or PHT-treated HL-60 cells were examined for morphological changes by light microscopy. To evaluate nuclear morphology, cells from cultures were harvested, transferred to cytospin slides, fixed with methanol for 30 s, and stained with hematoxylin–eosin.

*Cell membrane integrity.* The cell membrane integrity was evaluated by the exclusion of propidium iodide (2 μg/ml, Sigma Chemical Co. St Louis, MO, USA). Cell fluorescence was determined by flow cytometry in a Guava EasyCyte Mini System cytometer using the CytoSoft 4.1 software (Guava Technologies, Hayward, California, USA). Five thousand events were evaluated per experiment and cellular debris was omitted from the analysis.

*Cell cycle distribution and internucleosomal DNA fragmentation analysis.* The cells were harvested in a lysis solution containing 0.1% citrate, 0.1% Triton X-100, and 50 μg/ml propidium iodide (Nicoletti et al., 1991). Cell fluorescence was determined by flow cytometry as described above.

*Measurement of mitochondrial transmembrane potential.* Mitochondrial transmembrane potential was determined by the retention of the dye rhodamine 123 (Gorman et al., 1997; Sureda et al., 1997). Cells were washed with PBS, incubated with rhodamine 123 (5 μg/ml, Sigma Chemical Co. St Louis, MO, USA) at 37 °C for 15 min in the dark, and washed twice. The cells were then incubated again in PBS at 37 °C for 30 min in the dark and fluorescence was then measured by flow cytometry as described above.

*Annexin assay.* Phosphatidylserine externalization was analyzed by flow cytometry (Vermes et al., 1995). A Guava® Nexin Assay Kit (Guava Technologies, Hayward, CA) was used to determine apoptotic cells (early apoptotic +late apoptotic). Cells were washed twice with cold PBS and then re-suspended in 135 μl of PBS with 5 μl of 7-amino-actinomycin D (7-AAD) and 10 μl of Annexin V–PE. The cells were gently vortexed and incubated for 20 min at room temperature (20–25 °C) in the dark. Afterwards, the cells were analyzed by flow cytometry as described above.

*Caspase 3/7 and 8 activation.* Caspase 3/7 and 8 activity was analyzed by flow cytometry using the Guava® EasyCyte Caspase 3/7 and 8 Kits (Guava Technologies, Hayward, CA). The cells were incubated with Fluorescent Labeled Inhibitor of Caspases (FLICATM) and maintained for 1 h at 37 °C in a $CO_2$ incubator. After incubation, 80 μl of wash buffer was added and the cells were centrifuged at 2000 rpm for 5 min. The resulting pellet was resuspended in 200 μl of wash buffer and centrifuged again. The cells were then re-suspended in the working solution (propidium iodide and wash buffer) and analyzed immediately using flow cytometry as described above.

*Alkaline comet assay.* The alkaline (pH > 13) version of the comet assay (single cell gel electrophoresis) was performed as described by Singh et al. (1988) with minor modifications (Hartmann and Speit, 1997). Slides were prepared in duplicate, and 100 cells were screened per sample (50 cells from each duplicate slide), using a fluorescence microscope (Zeiss) equipped with a 515–560 nm excitation filter, a 590 nm barrier filter, and a 40× objective. Cells were scored visually according to tail length into five classes: (1) class 0: undamaged, without a tail; (2) class 1: with a tail shorter than the diameter of the head (nucleus); (3) class 2: with a tail length 1–2× the diameter of the head; (4) class 3: with a tail longer than 2× the diameter of the head; and (5) class 4: comets with no heads. A value of damage index (DI) was assigned to each comet according to its class, using the formula: $DI = (0 \times n_0) + (1 \times n_1) + (2 \times n_2) + (3 \times n_3) + (4 \times n_4)$, where $n$ = number of cells in each class analyzed. The damage index ranged from 0 (completely undamaged: 100 cells × 0) to 400 (with maxi–mum damage: 100 cells × 4). DI is based on migration length and on the amount of DNA in the tail, and it is considered a sensitive DNA measure (Speit and Hartmann, 1999).

*Tubulin polymerization assay.* With 96-well microplates sitting on ice, 25 μl of buffer A (80 mM PIPES, pH 6.8, 1 mM $MgCl_2$, 1 mM EGTA, and 10% glycerol) was added to the wells, followed by 15 μl of 10 mg/ml bovine brain tubulin (>99% pure, TL238 Cytoskeleton, Inc. Denver, CO) in buffer A containing 10% glycerol and 5 μl of 10 mM GTP. The absorbance at 340 nm was followed at 37 °C over time.

*Molecular modeling.* The docking of PHT into tubulin was performed using the version 4.0 of Autodock (Morris et al., 1998). The molecular model composed of tubulin monomers was previously published by Ravelli et al. (2004), based on crystallographic studies. The graphical interface AutoDockTools (Sanner et al., 1999) was also used to check molecular models, adding polar hydrogens (Kollman) and partial charges (Gasteiger), as well as to produce the appropriate parameter files and to analyze the results. Furthermore, the Å interface-associated programs were utilized to assign atomic solvation parameters for the protein and flexible torsions for the ligand. Autogrid (part of the Autodock package) allowed the construction of affinity grid fields, previously to the docking procedure.

Among the searching methods available in the package, we used the genetic algorithm and local search combined option. A whole tubulin dimer (α and β units) was considered in an earlier step (blind docking) for the affinity grid calculations, the grid field being divided into two sequential components, each one inside a 31.4 Å side cube, with grid points separated by 0.658 Å. For this step, the number of energy evaluations and docking runs were set to 2,500,000 and 10, respectively. All the other parameters were conserved as default. In a second step, the grid field was focused according to the docked molecule location obtained in the first step. This time, the grid cube allowed more precise measurements, with the grid points separated by 0.542 Å, centered on the best scored conformation observed in the first step. Accordingly, in the second step, the number of energy evaluations and docking runs were set to 25,000,000 and 50, respectively. Protein structure was considered rigid in all experiments. PHT structure was made flexible, with 6 rotatable bonds. At the end of the second step, we further investigated the region around the best docked conformation, within 5 Å and also within 3 Å of interaction distance, in order to find the closer residues. In a separated set of experiments, the protocol included a third step, designed to account for protein flexibility. This time, the lateral chains of residues situated within a 3 Å radius sphere, centered at the best scored conformation of PHT (interaction distance) obtained in step two, were also considered flexible.

The docking study was followed by an energy interaction investigation, using first principles, performed over the binding site. All amino acid residues situated within the 5 Å interaction distance, as well as PHT, were previously selected for the calculations. All atom coordinates in this region, except those of hydrogen, were kept frozen during the initialization stage. An optimization procedure, based on Molecular Mechanics, using Universal Force Field (UFF), was then applied to the hydrogen atoms only. For the Quantum Mechanical based simulations, we used Density Functional Theory, Local Density Approximation for the exchange-correlation functional, and a double numerical plus polarization basis set, using the software DMOL3 (Delley, 1990, 2000). The energy interactions between individual residues and RR07 were calculated according to the Molecular Fractionation Conjugate Caps (MFCC) formalism (Zhang and Zhang, 2003).

*Statistical analysis.* Data are presented as mean ± S.E.M. The $IC_{50}$ values were obtained by non-linear regression using the GRAPHPAD program (Intuitive Software for Science, San Diego, CA). Differences among experimental groups were compared by one-way analysis of variance (ANOVA) followed by Dunnett's test ($p < 0.05$).

## Results

### *PHT displayed cytotoxicity against different tumor cell lines*

Several tumor cell lines were treated with increasing concentrations of PHT for 72 h and analyzed by the MTT assay. PHT displayed cytotoxicity in all tumor cell lines, showing $IC_{50}$ values in the nanomolar range. Table 1 shows the obtained $IC_{50}$ values. Some $IC_{50}$ values previously published by us were also included. Doxorubicin was used as the positive control. Since HL-60 cells were especially sensitive to the antiproliferative effect of PHT, further studies were performed with this cell line.

**Table 1**
Cytotoxic effect of (4-methoxyphenyl)(3,4,5-trimethoxyphenyl)methanone (PHT) on tumor cell lines.

| Cell lines | Histotypes | PHT | Doxorubicin |
|---|---|---|---|
| B-16 | Melanoma | 0.72 | 0.05 |
| B-16-F10 | Melanoma | 0.40 | 0.07 |
| MDA-MB-435[a] | Melanoma | 0.21 | 0.83 |
| HL-60[a] | Leukemia | 0.13 | 0.03 |
| CEM | Leukemia | 0.19 | 0.03 |
| K-562 | Leukemia | 0.26 | 0.24 |
| JURKAT | Leukemia | 2.21 | Nd |
| MDA-MB-231 | Breast | 17.49 | 0.38 |
| MX-1 | Breast | 3.01 | 0.13 |
| PC-3 | Prostate | 2.68 | 0.41 |
| HCT-8[a] | Colon | 0.40 | 0.07 |
| S180[a] | Sarcoma | 0.29 | 0.23 |
| SF-295[a] | Glioblastoma | <0.03 | 0.40 |
| PBMC[b] | Normal lymphocyte | 5.68 | 1.78 |

Data are presented as $IC_{50}$ values (μM) from two independent experiments performed in duplicate measured by the MTT assay after 72 h incubation. Doxorubicin was used as the positive control. Nd: not determined.
[a] Published by Magalhães et al.(2011a).
[b] Published by Magalhães et al. (2011b).

A cell viability curve was determined by trypan blue dye exclusion method after 3, 6, 12, 18, and 24 h incubation. PHT reduced the cell number in a concentration- and time-dependent manner (Fig. 2A). Compared to the control, a decrease in the number of cells was observed within the first 12 h of incubation at all tested concentrations ($p < 0.05$). In order to get additional understanding of the antiproliferative effect of PHT, experiments were conducted after 24 h incubation, at concentrations that ranged from 0.25 to 5.0 μM.

As observed using trypan blue dye exclusion (Fig. 2B), BrdU incorporation (Fig. 2C), and propidium iodide exclusion (Fig. 2D), PHT reduced the cell number, after 24 h incubation, at all tested concentrations ($p < 0.05$). In cell viability assay determined by trypan blue dye exclusion method, PHT reduced the number of viable cells by 30%, 37%, and 44% at the concentrations of 0.25, 0.5, and 1.0 μM, respectively. When the cell viability was determined by flow cytometry using propidium iodide, the inhibitions were 64%, 66%, and 67% at the same concentrations. In cell proliferation assay determined by incorporation of the nucleotide BrdU, the inhibitions were 59%, 80%, and 86% at the same concentrations.

*PHT treatment induces cell cycle arrest in HL-60 human leukemia cells*

To further investigate the mechanisms involved in the cytotoxic activity, the effect of PHT was evaluated on the cell cycle progression using flow cytometry. Table 2 shows the obtained cell cycle distribution. PHT treatment, at all concentrations, resulted in a significantly increase in the number of cells in $G_2$/M phase compared to the negative control ($p < 0.05$). On control, the percentage of cells corresponding to $G_0/G_1$ phases was 33%, to S phase was 57%, and to $G_2$/M phases was 10%. Cells with internucleosomal DNA fragmentation (sub-$G_1$) corresponded to 6%. For PHT-treated cells the percentage of cells corresponding to $G_2$/M was 57%, 52%, and 51% at concentrations of 0.25, 0.5, and 1.0 μM, respectively. Besides the increasing of cells in $G_2$/M, a decreasing of cells in $G_0/G_1$ and an increasing in the internucleosomal DNA fragmentation were also observed ($p < 0.05$, Fig. 4B). Herein, doxorubicin led preferentially cancer cells from $G_2$/M phases to DNA fragmentation. Doxorubicin also can induce $G_2$/M arrest, which depends on the drug concentration, time of exposure and cell line used.

**Table 2**
Effect of (4-methoxyphenyl)(3,4,5-trimethoxyphenyl)methanone (PHT) on the cell cycle distribution of HL-60 human leukemia cells after 24 h incubation.

| Drug | Concentration (μM) | Cell cycle phase (%) | | |
|---|---|---|---|---|
| | | $G_0/G_1$ | S | $G_2$/M |
| NC | – | 33.1 ± 3.6 | 57.2 ± 4.2 | 9.7 ± 1.0 |
| PC | 0.5 | 32.3 ± 2.4 | 65.9 ± 2.7 | 1.8 ± 0.5 |
| PHT | 0.25 | 9.7 ± 1.6* | 33.1 ± 8.2* | 57.3 ± 6.7* |
| | 0.5 | 10.7 ± 1.6* | 37.8 ± 7.0 | 51.5 ± 5.3* |
| | 1.0 | 9.3 ± 1.7* | 39.4 ± 8.4 | 51.3 ± 6.9* |

Negative control (NC) was treated with the vehicle used for diluting the tested substance. Doxorubicin was used as the positive control (PC). Data are presented as mean values ± S.E.M. from three independent experiments performed in duplicate. Five thousand events were analyzed in each experiment. Each phase was calculated using the cell ModFIT program.
* $p < 0.05$ compared to control by ANOVA followed by Dunnett's test.

Additionally, morphological changes were investigated using hematoxylin–eosin staining. PHT caused an increase in the mitotic figures in metaphase stage (Figs. 3E and F). These results support that there is a mitotic arrest associated with PHT treatment.

*PHT treatment induces apoptosis in HL-60 human leukemia cells*

In addition to increase in the mitotic figures, morphological examination of HL-60 cells showed severe drug-mediated changes (Fig. 3). HL-60 cells treated with PHT, at all tested concentrations, presented

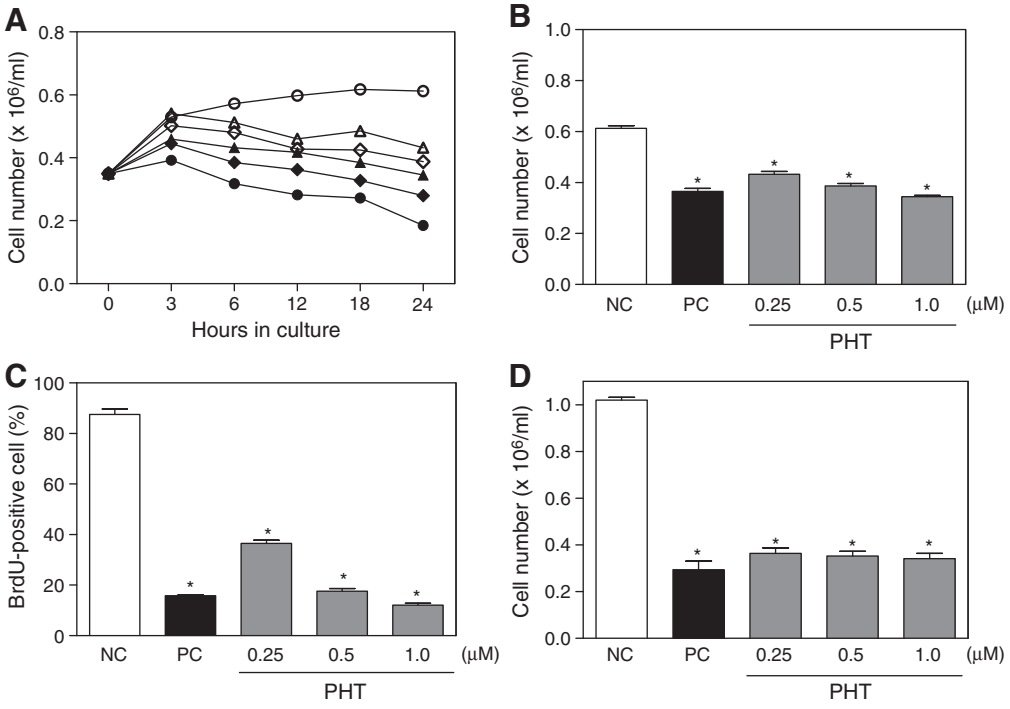


**Fig. 2.** Effect of (4-methoxyphenyl)(3,4,5-trimethoxyphenyl)methanone (PHT) on viability/proliferation of HL-60 human leukemia cells. (A) Cell viability curve determined by trypan blue dye exclusion method. (B) Cell viability determined by trypan blue dye exclusion method after 24 h incubation. (C) Cell proliferation determined by incorporation of the nucleotide BrdU after 24 h incubation. (D) Cell viability determined by flow cytometry using propidium iodide after 24 h incubation. Negative control (NC) was treated with the vehicle (0.1% DMSO) used for diluting the tested substance. Doxorubicin (0.5 μM) was used as the positive control (PC). Data are presented as mean values ± S.E.M. from three independent experiments performed in duplicate. For flow cytometric analysis five thousand events were analyzed in each experiment. *, $p < 0.05$ compared to negative control by ANOVA followed by Dunnett's test.

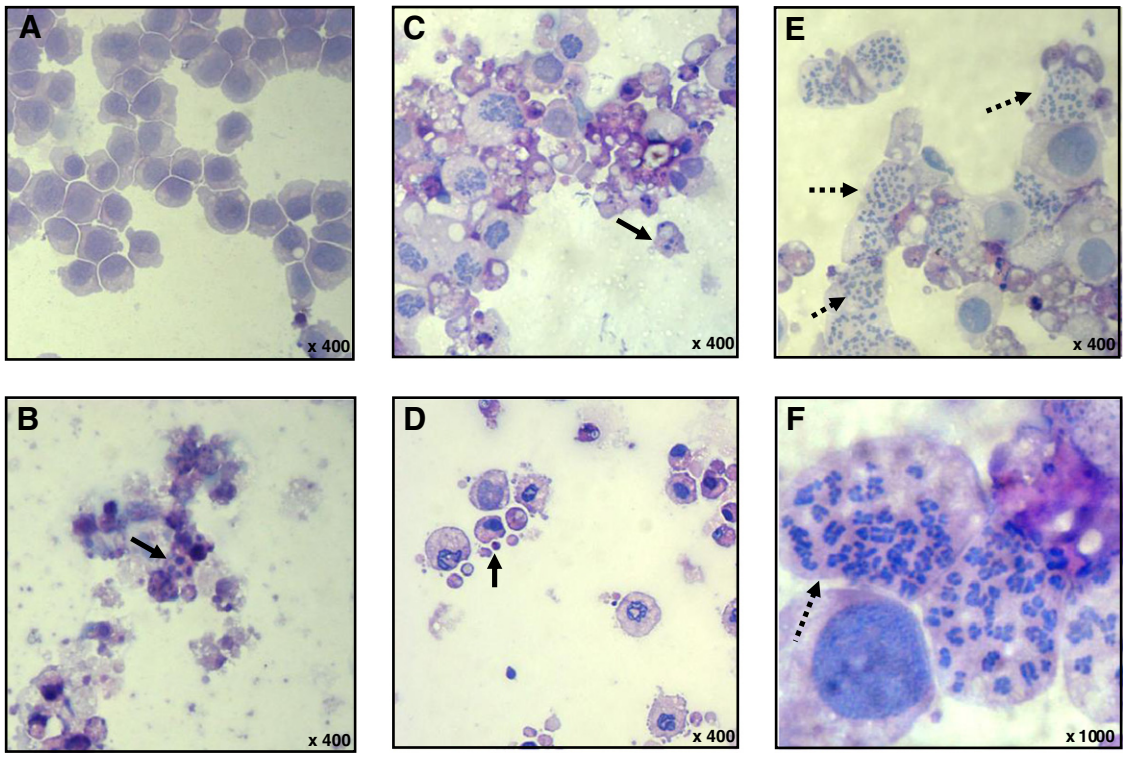


**Fig. 3.** Effect of (4-methoxyphenyl)(3,4,5-trimethoxyphenyl)methanone (PHT) on cell morphology of HL-60 human leukemia cells. The cells were stained with hematoxylin–eosin and analyzed by optical microscopy after 24 h incubation with PHT at concentrations 0.25 (C), 0.5 (D), and 1.0 μM (E and F). Negative control (A) was treated with the vehicle (0.1% DMSO) used for diluting the tested substance. Doxorubicin (0.5 μM) was used as the positive control (B). Continuous arrows show nuclear fragmentation and non-continuous arrows show accumulation of metaphases cells.

morphology consistent with apoptosis, including reduction in cell volume, chromatin condensation, and fragmentation of the nuclei. Doxorubicin also induced cell shrinkage, chromatin condensation, and nuclear fragmentation, morphology consistent with apoptosis.

The cell membrane integrity serves as a parameter of the viability of treated and untreated HL-60 cells. After 24 h of exposure, PHT did not disrupt membrane at any tested concentration ($p > 0.05$, Fig. 4A). As cited above, DNA fragmentation markedly increased in PHT-treated cells and was present in more than 60% of treated cells ($p < 0.05$, Fig. 4B). Both of these modifications were compatible with apoptotic cells. In addition, the alkaline comet assay was used to evaluate induction of DNA damage (single-strand and double-strand breaks). Fig. 4C shows the effect of PHT on the damage index, as measured by effects on DNA. At 2.0 and 4.0 μM, PHT clearly produced a significant increase in damage index as compared to the control groups ($p < 0.05$). Phosphatidylserine externalization of PHT-treated cells was also measured by flow cytometry using annexin assay. Since externalization of phosphatidylserine occurs in the earlier stages of apoptosis, annexin V staining can identify apoptosis at an earlier stage than assays based on nuclear changes such as DNA fragmentation. In addition, propidium iodide and annexin V staining are widely used assays to detect apoptotic and necrotic cells. PHT treatment induced an increase of the percentage of apoptotic cells ($p < 0.05$, Fig. 4D). Doxorubicin, used as the positive control, also induced phosphatidylserine exposure and DNA fragmentation without affecting membrane integrity.

To determine whether PHT-treated cells were truly undergoing an apoptotic death, mitochondrial transmembrane potential and caspase 3/7 and 8 activation were measured by flow cytometry. PHT induced mitochondrial depolarization in HL-60 cells, as measured by incorporation of rhodamine-123, suggesting intrinsic mitochondrial-dependent apoptosis cell death. The mitochondrial depolarization occurred at all tested concentrations ($p < 0.05$, Fig. 5A). Additionally, caspase 3/7 and 8 activation was increased in PHT-treated cells ($p < 0.05$, Figs. 5B and C). The increase of the caspase 3/7 and 8 activation also suggests extrinsic apoptosis pathway.

*PHT treatment caused inhibitory effect on tubulin polymerization*

To insight into the mechanism of action of PHT, we examined its effect on the polymerization of pure tubulin into microtubules *in vitro*. Purified brain tubulin (3 mg/ml) was pre-incubated with DMSO, nocodazole or PHT on ice, and the temperature was raised to 37 °C. Microtubules polymerized spontaneously in the presence of DMSO, whereas nocodazole (10 μM), a known inhibitor of tubulin polymerization, completely blocked their assembly. PHT (10 μM) also inhibited the assembly of microtubules (Fig. 6). The inhibition percentages were 33% and 42%, respectively.

To better understand the interaction between tubulin and PHT, molecular docking was performed by simulation of PHT into the colchicine binding site in tubulin. The binding model of PHT and tubulin was depicted in Fig. 7. Analysis of the clusters formed in the second step of the approach showed PHT docked conformations placed mainly in the region situated close to the interface between β and α subunits, as indicated by the conformation shown in Fig. 7A. Then, we focused our studies in the same place that has been suggested by Ravelli et al. (2004) being the region of tubulin that is preferred by colchicine (Fig. 7B). The lowest energy conformation found in this case was −6.90 kcal/mol.

The more flexible docking in the third step produced a still lower binding energy (−9.17 kcal/mol), indicating a possible role for the lateral chains of the protein residues located around the docked PHT. Future studies are necessary to clarify this point. The best scored conformation obtained after some second step experiments was then investigated for additional information in this site. We first adopted a possible interaction distance of 5 Å, within which there are atoms (at least one) of the following residues (Fig. 7C). From α unit: ASN101,

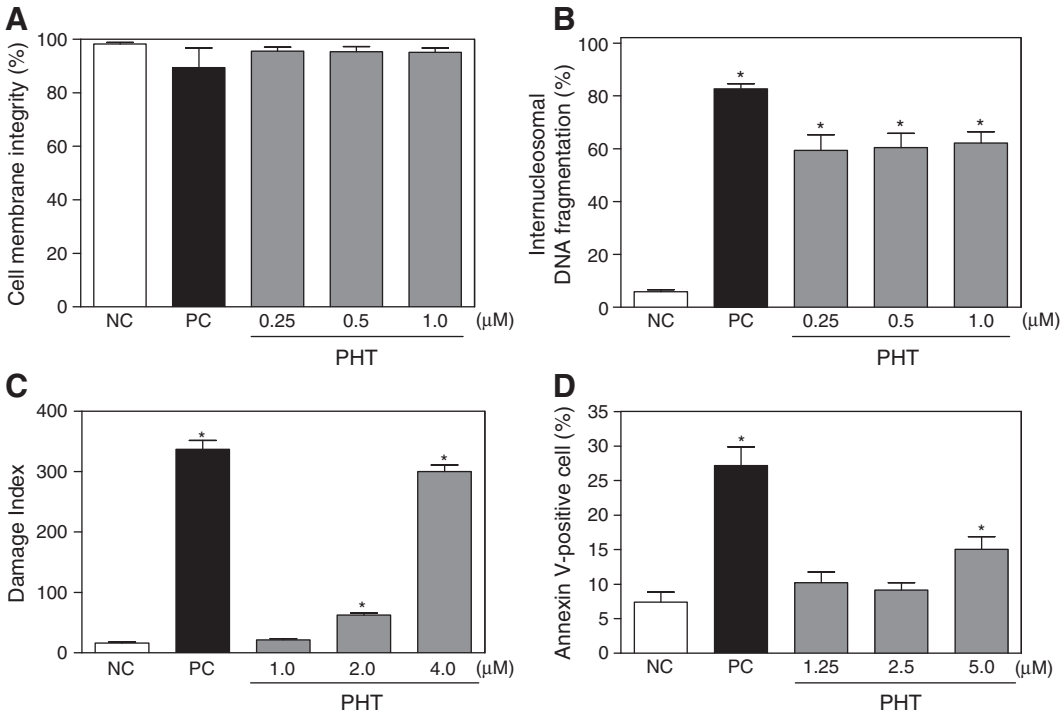


**Fig. 4.** Effect of (4-methoxyphenyl)(3,4,5-trimethoxyphenyl)methanone (PHT) on viability of HL-60 human leukemia cells after 24 h incubation. (A) Cell membrane integrity determined by flow cytometry using propidium iodide. (B) Internucleosomal DNA fragmentation determined by flow cytometry using propidium iodide and triton X-100. (C) DNA damage determined by alkaline comet assay. (D) Cell viability determined by flow cytometric using Annexin V–PE. Negative control (NC) was treated with the vehicle (0.1% DMSO) used for diluting the tested substance. Doxorubicin (0.5 μM) was used as the positive control (PC). Data are presented as mean values ± S.E.M. from three independent experiments performed in duplicate. For flow cytometric analysis five thousand events were analyzed in each experiment. *, $p < 0.05$ compared to negative control by ANOVA followed by Dunnett's test.

THR179, and ALA180; from β unit: TYR202, VAL238, THR239, CYS241, LEU242, LEU248, ASN249, ALA250, ASP251, LEU252, ARG253, LYS254, LEU255, ALA256, ASN258, ALA316, ALA317, VAL318, LYS352, ALA354, and ILE378. We later submitted the above system (within interaction distance of 5 Å) to the MFCC formalism, in order to obtain the interaction energies between those residues and PHT. The major interactions (in module), i.e., those with most influence in ligand stability, were between PHT and the following residues (from β unit): LEU248, ALA250, LYS254, and LEU255, with values for interaction energy of −53.00, −22.00, −26.00, and −32.00 kcal/mol, respectively. The main contributors to PHT stability in the binding site were emphasized in Fig. 7D.

The residues LEU β 248, ALA β 250, and LEU β 255 have strong hydrophobic interactions with the ligand, while LYS β 254 has an electrostatic interaction between its $NH_3$ functional group and one of ligand's methoxy groups.

## Discussion

The purpose of the current study was to investigate the mechanisms underlying PHT-induced cytotoxicity. Previous works have been reported that PHT displayed high potency in the inhibition of tubulin polymerization and cytotoxicity against several cancer cell lines. In this study, for the first time, a serial protocol was performed in PHT-treated HL-60 human leukemia cells to characterize its effects on cell proliferation, cell cycle progress, and apoptosis induction. Studies in purified tubulin and molecular docking were performed to confirm the interference of PHT in the polymerization of microtubules.

PHT displayed cytotoxicity in several of tumor cell lines, showing $IC_{50}$ values in the nanomolar range. The inhibitory effect of PHT on tumor cell proliferation was determined by colorimetric method using MTT assay, trypan blue dye exclusion method, detection of incorporation of the nucleotide BrdU through immunocytochemistry, and flow cytometry using propidium iodide exclusion. PHT affected the cell proliferation in a concentration- and time-dependent manner. These data have been reported previously by different research groups (Alvarez et al., 2009; Cushman et al., 1992; Liou et al., 2002; Magalhães et al., 2011a). In all studies its high cytotoxicity against tumor cell line (nanomolar range) has been one of its highlights. In the preclinical anticancer drug-screening program, the lead compounds that show $IC_{50}$ values below 1 μM are considered promising (Bezerra et al., 2008; Costa-Lotufo et al., 2004; Pessoa et al., 2000). Therefore, PHT can be considered a very potent cytotoxic compound. In addition, its cytotoxicity against normal lymphocyte (PBMC) was less pronounced ($IC_{50}$ = 5.68 μM) (Magalhães et al., 2011b). The Selectivity Index (SI, where SI = $IC_{50}$[PBMC] / $IC_{50}$[HL-60]) for HL-60 human leukemia cells was 44 and 59 for PHT and doxorubicin, respectively.

The effect of PHT on cell proliferation was cell cycle specific. Cell cycle arrest in $G_2$/M phases was found in PHT-treated cells. In addition, the cells also displayed morphological features that identified a mitotic arrest, specifically in metaphase. The ability of PHT to arrest cancer cells in $G_2$/M phases is consistent with cytotoxic agents that act by binding to tubulin. The compounds that damage mitotic spindles inhibit the tumor cell proliferation and block cells at metaphase phase (Cocca et al., 2009; Prinz et al., 2003, 2011; Rycker et al., 2009; Schneider et al., 2003). The hypothesis that arrest of the cell cycle at mitosis is following by apoptosis has been largely accepted. Moreover, several tubulin-binding agents kill cancer cells primarily by apoptosis. Further, the mechanism of apoptotic cell death was also investigated in PHT-treated cells.

Apoptosis plays an important role in a variety of biological events, including development and removal of unwanted harmful cells. Apoptosis is a largely regulated form of cell death and its deregulation results in several pathological conditions including cancer, autoimmune, and neurodegenerative diseases. Therefore, induction of apoptosis is an important target for cancer therapy (Fesik, 2005; Ghobrial et al.,

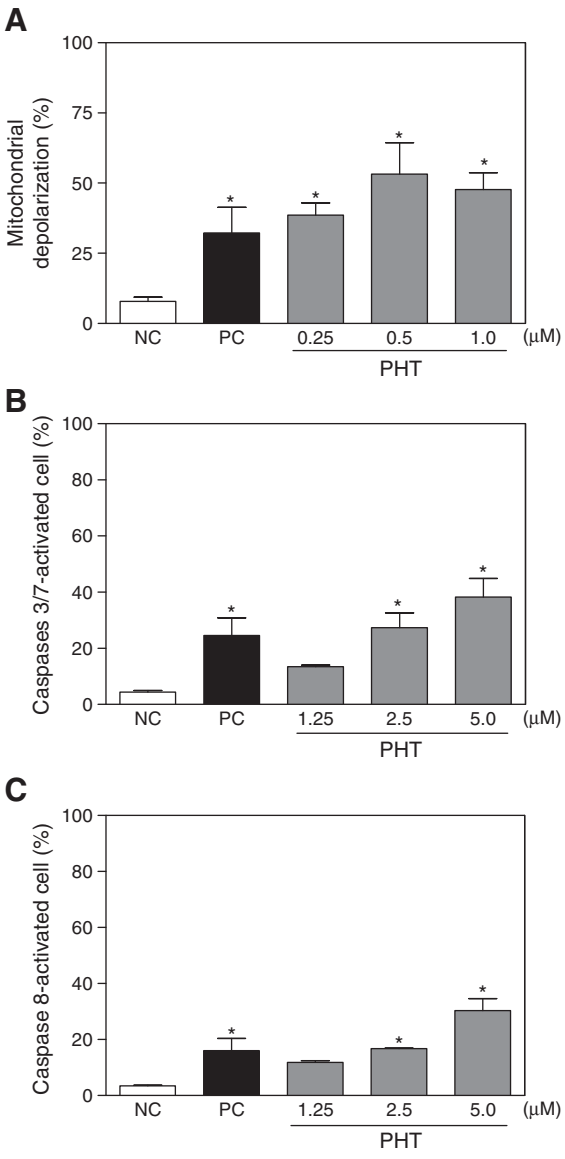


**Fig. 5.** Effect of (4-methoxyphenyl)(3,4,5-trimethoxyphenyl)methanone (PHT) on viability of HL-60 human leukemia cells after 24 h incubation. (A) Mitochondrial membrane potential determined by flow cytometry using rhodamine 123. (B) Activity of caspases 3/7 determined by flow cytometry using propidium iodide and Flica. (C) Activity of caspase 8 determined by flow cytometry using propidium iodide and Flica. Negative control (NC) was treated with the vehicle (0.1% DMSO) used for diluting the tested substance. Doxorubicin (0.5 μM) was used as the positive control (PC). Data are presented as mean values ± S.E.M. from three independent experiments performed in duplicate. For flow cytometric analysis five thousand events were analyzed in each experiment. *, $p < 0.05$ compared to negative control by ANOVA followed by Dunnett's test.

2005; Ola et al., 2011). Changes typical for apoptosis including reduction in cell volume, chromatin condensation, phosphatidylserine exposure, internucleosomal DNA fragmentation without affecting membrane integrity, caspase 3/7 and 8 activation, and loss of mitochondrial membrane potential were observed in PHT-treated cells.

Apoptotic cell death is independent or dependent on a family of aspartate specific cysteine proteases (caspases) that cleave certain vital structural proteins (*e.g.*, lamins, gelsolin) and proteolytically activate latent enzymes (*e.g.*, nucleases) that contribute to cell death. In mammals, caspase-dependent apoptosis occurs through two main interconnected pathways: intrinsic and extrinsic (Cande et al., 2002; Comelli et al., 2009; Ola et al., 2011). The extrinsic pathway is initiated by death receptors (*e.g.*, FAS and tumor necrosis factor-α [TNF-α]) on the cell surface. Interaction of a death receptor with its ligand triggers the formation of a death-inducing signaling complex, which in turn recruits procaspase 8. Pro-caspase 8 undergoes autoproteolytic cleavage, forming active caspase 8, an initiator caspase of the extrinsic pathway (Lavrik et al., 2005; Ola et al., 2011). In the present study, we found that an increase of the caspase 8 activation in PHT-treated cells suggests that extrinsic pathway is involved. The intrinsic pathway is initiated with loss of membrane potential in mitochondria and then the release of cytochrome c from the mitochondria into the cytosol and binding to the adaptor protein Apaf-1 following activation of caspase 9, an initiator caspase of the intrinsic pathway. In both pathways, the activated initiator caspase leads to their own autoactivation which further activates the caspase 3 and caspase 7, effector caspases (Brenner and Kroemer, 2000; Ola et al., 2011; Saelens et al., 2004). The loss of mitochondrial membrane potential observed after PHT treatment exhibits the involvement of intrinsic pathway in PHT-induced cell death. Furthermore, increase of the caspase 3/7 activation was also observed in PHT-treated cells. These dates show that both the extrinsic signaling pathway and the intrinsic signaling pathway would appear to contribute to PHT-induced apoptosis.

Anyway, apoptosis is not the only mechanism of tubulin inhibitor-induced cell death. Several studies have described a form of cell death called mitotic catastrophe. Mitotic catastrophe is an event in which a cell is destroyed during mitosis. It occurs because of an attempt at aberrant chromosome segregation in mitosis or as a result of DNA damage (Castedo et al., 2004; Mollinedo and Gajate, 2003). It has been reported that tubulin-binding agents induce cell death through a mitotic catastrophe (Kanthou et al., 2004; Nabha et al., 2002). Interestingly, Magalhães et al. (2011b) showed that PHT also is able to induce an accumulation of metaphase cells on cultured lymphocytes. Moreover, a considerable increase in the frequency of chromosome aberrations was found in cells exposed to PHT. This genotoxic effect can be important as an alternative strategy for PHT to induce cancer cell death.

Studies with CA-4 analogs have been shown similar results. Nabha et al. (2000) demonstrated that CA-4 may induce $G_2$/M arrest, mitotic catastrophe, and apoptotic cell death in a panel of malignant human B-lymphoid cell lines. Petit et al. (2008) showed that combretastatin-A4-phosphate (CA-4P) inhibits leukemic cell proliferation *in vitro* and induces mitotic arrest and cell death. Treatment of leukemia cells with CA-4P leads to disruption of mitochondrial membrane potential, release of proapoptotic mitochondrial membrane proteins, and DNA fragmentation, resulting in cell death through a caspase-dependent manner. Moreover, CA-4P increases intracellular reactive oxygen species (ROS) suggesting that ROS accumulation contributes to CA4P-induced cytotoxicity.

As previously cited tubulin targeting drugs typically bind to one of three sites on tubulin: the taxane, the vinca or the colchicine sites (Buey et al., 2005; Dumontet and Jordan, 2010; Jordan and Kamath, 2007; Lobert et al., 1999). Phenstatins are able to bind to the colchicine site (Pettit et al., 1998). In fact, some studies have been proposed that PHT inhibits tubulin polymerization through binding to the colchicine site. Barbosa et al. (2009), using [$^3$H] colchicine binding assay, showed that PHT is able to inhibit the colchicine binding in 78% at the concentration of 5 μM; the same concentration of CA-4 inhibits 99%. In addition, both, PHT and CA-4, are able to inhibit tubulin polymerization in micromolar range, the estimated $IC_{50}$ value was 7.4 and 2.0 μM for PHT and CA-4, respectively (Alvarez et al., 2009; Barbosa et al., 2009; Cushman et al., 1992). Herein, using isolated tubulin, we confirmed that PHT is a tubulin inhibitor.

Molecular dock was performed to confirm the binding of PHT to the colchicine site. Docking approaches have been contributed to the development of models able to explain the structure–activity relationships of numerous types of tubulin inhibitors (Botta et al., 2009). In our docking models, the similarity of the present findings can be seen by superposing our coordinates to the colchicine-docked conformation from a previous study produced by Ravelli et al. (2004). We identified that

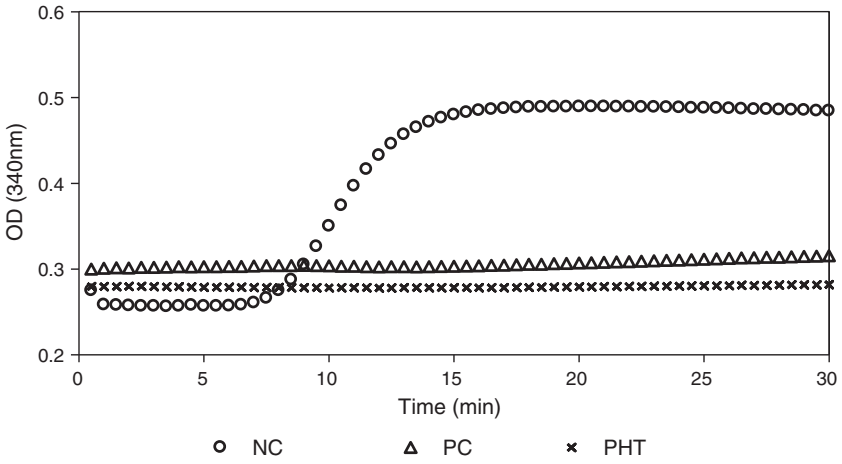


**Fig. 6.** Effect of (4-methoxyphenyl)(3,4,5-trimethoxyphenyl)methanone (PHT) on microtubule polymerization. Microtubule polymerization was carried out with 3 mg/ml tubulin in 10 μM PHT. Negative control (NC) was treated with the vehicle (DMSO) used for diluting the tested substance. Nocodazole (10 μM) was used as the positive control (PC).

the residues LEU β 248, ALA β 250, and LEU β 255 have strong hydrophobic interactions with the ligand, while LYS β 254 has an electrostatic interaction between its $NH_3$ functional group and one of ligand's methoxy groups. For colchicine, the residues SER α 178, THR α 179, VAL α 181, CYS β 241, and LYS β 352 are involved, while the residues THR α 179, VAL α 181, and CYS β 241 are involved for CA-4 (Bellina et al., 2006; Kong et al., 2005; Nguyen et al., 2005; Rappl et al., 2006). Alvarez et al. (2009) also had docked PHT in a combined podophyllotoxin–colchicine site. They concluded that 3-X-4-methoxyphenyl rings superimpose onto the methylenedioxyphenyl ring of podophyllotoxin. Moreover, the prediction that the carbonyl oxygen of phenstatins can act as a hydrogen bond acceptor pharmacophoric point additional to those found in combretastatins was confirmed.

In summary, our data presents that PHT-induced cytotoxicity is based on its ability to bind to colchicine site on tubulin (Fig. 8). As a consequence, PHT inhibits tubulin polymerization, arrests cancer cells in

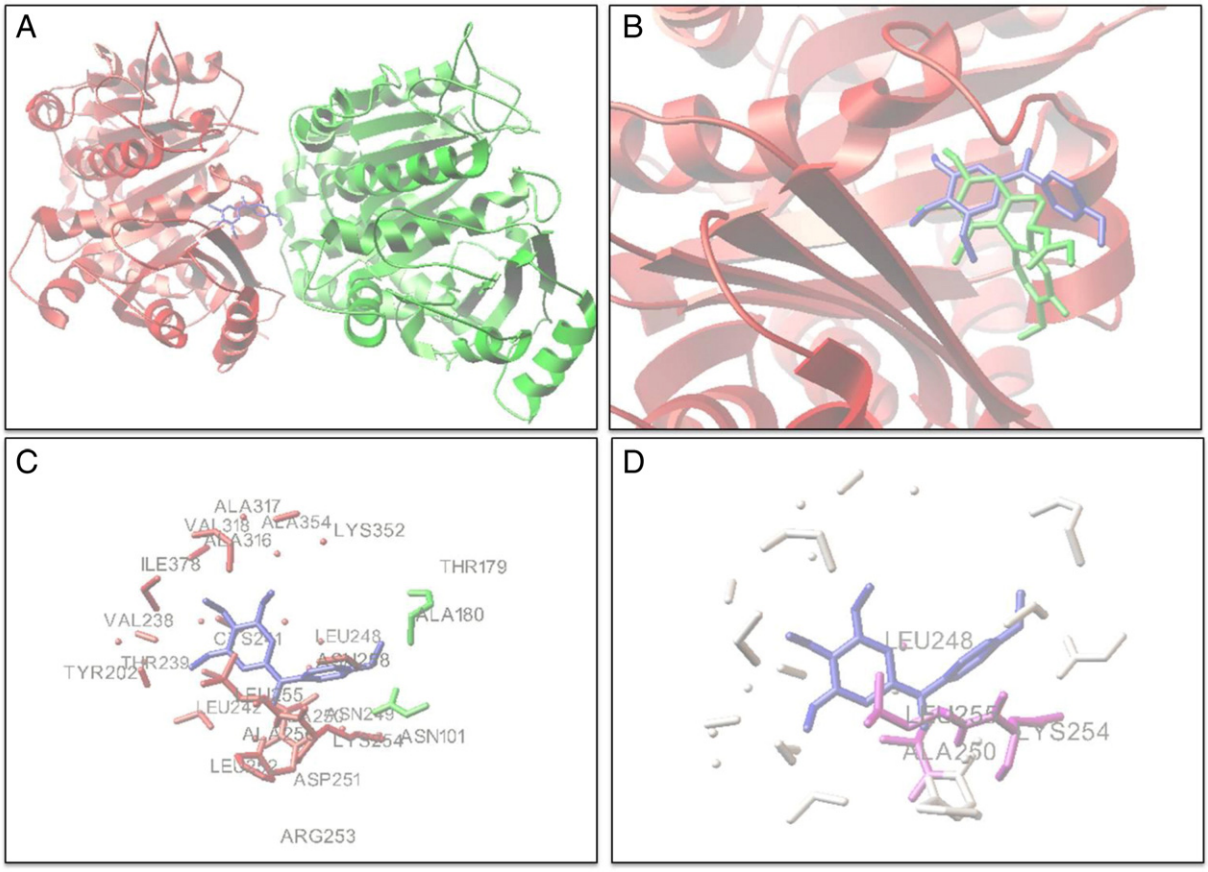


**Fig. 7.** The molecular docking model of PHT with tubulin. (A) PHT (blue) docked in the interface between tubulin α (green) and β (red) units. (B) A closer view of docked PHT (blue). For comparison, colchicine cords were superposed (green). (C) Residues with at least one atom within interaction distance of 5 Å from PHT (blue). (D) Residues (magenta) with major contribution within interaction distance of 5 Å to PHT (blue) stability.

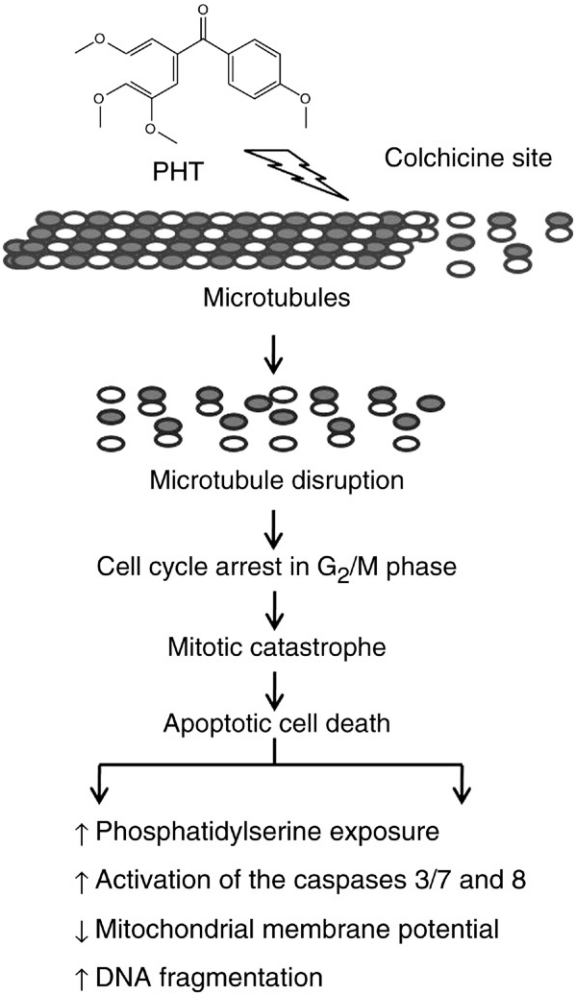


**Fig. 8.** The proposed mechanism of the action of (4-methoxyphenyl)(3,4,5-trimethoxyphenyl)methanone (PHT). PHT promoted inhibition of tubulin polymerization followed by $G_2$/M phase arrest and caspase-dependent apoptosis death in human leukemia cell.

$G_2$/M phase of the cell cycle, and induces caspase-dependent apoptosis in human leukemia cell, exhibiting promising anticancer therapeutic potential.

## Conflicts of interest

The authors declare no conflicts of interest.

## Acknowledgments

We wish to thank CNPq, CAPES, Instituto Claude Bernard, FUNCAP, PROPP (UFMS), FUNDECT (MS), and FINEP for their financial support in the form of grants and fellowship awards. The authors also thank the National Cancer Institute (Bethesda, MD, USA) for the donation of the tumor cell lines used in this study. The authors thank Silvana França dos Santos, Luciana França, and Maria de Fátima Teixeira for technical assistance.

## References

Alvarez, C., Alvarez, R., Corchete, P., Pérez-Melero, C., Peláez, R., Medarde, M., 2008. Naphthylphenstatins as tubulin ligands: synthesis and biological evaluation. Bioorg. Med. Chem. 16, 8999–9008.

Alvarez, R., Alvarez, C., Mollinedo, F., Sierra, B.G., Medarde, M., Peláez, R., 2009. Isocombretastatins A: 1,1-diarylethenes as potent inhibitors of tubulin polymerization and cytotoxic compounds. Bioorg. Med. Chem. 17, 6422–6431.

Alvarez, C., Alvarez, R., Corchete, P., Pérez-Melero, C., Peláez, R., Medarde, M., 2010. Exploring the effect of 2,3,4-trimethoxy-phenyl moiety as a component of indolephenstatins. Eur. J. Med. Chem. 45, 588–597.

Barbosa, E.G., Bega, L.A.S., Beatriz, A., Sarkar, T., Hamel, E., Amaral, M.S., Lima, D.P., 2009. A diaryl sulfide, sulfoxide, and sulfone bearing structural similarities to combretastatin A-4. Eur. J. Med. Chem. 44, 2685–2688.

Bellina, F., Cauteruccio, S., Monti, S., Rossi, R., 2006. Novel imidazole-based combretastatin A-4 analogues: evaluation of their *in vitro* antitumor activity and molecular modeling study of their binding to the colchicine site of tubulin. Bioorg. Med. Chem. Lett. 16, 5757–5762.

Bezerra, D.P., Pessoa, C., Moraes, M.O., Alencar, N.M., Mesquita, R.O., Lima, M.W., Alves, A.P., Pessoa, O.D., Chaves, J.H., Silveira, E.R., Costa-Lotufo, L.V., 2008. *In vivo* growth inhibition of sarcoma 180 by piperlonguminine, an alkaloid amide from the *Piper* species. J. Appl. Toxicol. 28, 599–607.

Botta, M., Forli, S., Magnani, M., Manetti, F., 2009. Molecular modeling approaches to study the binding mode on tubulin of microtubule destabilizing and stabilizing agents. Top. Curr. Chem. 286, 279–328.

Brenner, C., Kroemer, G., 2000. Apoptosis: mitochondria — the death signal integrators. Science 289, 1150–1151.

Buey, R.M., Barasoain, I., Jackson, E., Meyer, A., Giannakakou, P., Paterson, I., Mooberry, S., Andreu, J.M., Díaz, J.F., 2005. Microtubule interactions with chemically diverse stabilizing agents: thermodynamics of binding to the paclitaxel site predicts cytotoxicity. Chem. Biol. 12, 1269–1279.

Cande, C., Cecconi, F., Dessen, P., Kroemer, G., 2002. Apoptosis inducing factor (AIF): key to the conserved caspase-independent pathways of cell death? J. Cell Sci. 115, 4727–4734.

Castedo, M., Perfettini, J.L., Roumier, T., Andreau, K., Medema, R., Kroemer, G., 2004. Cell death by mitotic catastrophe: a molecular definition. Oncogene 23, 2825–2837.

Cocca, C., Dorado, J., Calvo, E., López, J.A., Santos, A., Perez-Castillo, A., 2009. 15-Deoxi-D12,14-prostaglandin J2 is a tubulin-binding agent that destabilizes microtubules and induces mitotic arrest. Biochem. Pharmacol. 78, 1330–1339.

Comelli, M., Genero, N., Mavelli, I., 2009. Caspase-independent apoptosis in Friend's erythroleukemia cells: role of mitochondrial ATP synthesis impairment in relocation of apoptosis-inducing factor and endonuclease G. J. Bioenerg. Biomembr. 41, 49–59.

Costa-Lotufo, L.V., Silveira, E.R., Barros, M.C., Lima, M.A., De Moraes, M.E., De Moraes, M.O., Pessoa, C., 2004. Antiproliferative effects of abietane diterpenes from *Aegiphila lhotzkyana*. Planta Med. 70, 180–182.

Cushman, M., Nagarathnam, D., Gopal, D., He, H.M., Lin, C.M., Hamel, E., 1992. Synthesis and evaluation of analogs of (Z)-1-(4-methoxyphenyl)-2-(3,4,5-trimethoxyphenyl) ethene as potential cytotoxic and antimitotic agents. J. Med. Chem. 35, 2293–2306.

Delley, B., 1990. An all-electron numerical method for solving the local density functional for polyatomic molecules. J. Chem. Phys. 92, 508–517.

Delley, B., 2000. From molecules to solids with the DMol3 approach. J. Chem. Phys. 113, 7756–7764.

Dumontet, C., Jordan, M.A., 2010. Microtubule-binding agents: a dynamic field of cancer therapeutics. Nat. Rev. Drug Discov. 9, 790–803.

Fesik, S.W., 2005. Promoting apoptosis as a strategy for cancer drug discovery. Nat. Rev. Cancer 5, 876–885.

Ghobrial, I.M., Witzig, T.E., Adjei, A.A., 2005. Targeting apoptosis pathways in cancer therapy. CA Cancer J. Clin. 55, 178–194.

Gorman, A.M., Samali, A., McGowan, A.J., Cotter, T.G., 1997. Use of flow cytometry techniques in studying mechanisms of apoptosis in leukemic cells. Cytometry 29, 97–105.

Hartmann, A., Speit, G., 1997. The contribution of cytotoxicity to DNA effects in the single cell gel test (comet assay). Toxicol. Lett. 90, 183–188.

Jordan, M.A., Kamath, K., 2007. How do microtubule targeted drugs work? An overview. Curr. Cancer Drug Targets 7, 730–742.

Kanthou, C., Greco, O., Stratford, A., Cook, I., Knight, R., Benzakour, O., Tozer, G., 2004. The tubulin-binding agent combretastatin A-4-phosphate arrests endothelial cells in mitosis and induces mitotic cell death. Am. J. Pathol. 165, 1401–1411.

Kong, Y., Grembecka, J., Edler, M.C., Hamel, E., Mooberry, S.L., Sabat, M., Rieger, J., Brown, M.L., 2005. Structure-based discovery of a boronic acid bioisostere of combretastatin A-4. Chem. Biol. 12, 1007–1014.

Lavrik, I., Golks, A., Krammer, P.H., 2005. Death receptor signaling. J. Cell Sci. 118, 265–267.

Liou, J.P., Chang, C.W., Song, J.S., Yang, Y.N., Yeh, C.F., Tseng, H.Y., Lo, Y.K., Chang, Y.L., Chang, C.M., Hsieh, H.P., 2002. Synthesis and structure–activity relationship of 2-aminobenzophenone derivatives as antimitotic agents. J. Med. Chem. 45, 2556–2562.

Liou, J.P., Chang, J.Y., Chang, C.W., Chang, C.Y., Mahindroo, N., Kuo, F.M., Hsieh, H.P., 2004. Synthesis and structure–activity relationships of 3-aminobenzophenones as antimitotic agents. J. Med. Chem. 47, 2897–2905.

Lobert, S., Ingram, J.W., Correia, J.J., 1999. Additivity of dilantin and vinblastine inhibitory effects on microtubule assembly. Cancer Res. 59, 4816–4822.

Magalhães, H.I., Bezerra, D.P., Cavalcanti, B.C., Wilke, D.V., Rotta, R., Lima, D.P., Beatriz, A., Alves, A.P.N.N., Bitencourt, F.S., Figueiredo, I.S.T., Alencar, N.M.N., Costa-Lotufo, L.V., Moraes, M.O., Pessoa, C., 2011a. *In vitro* and *in vivo* antitumor effects of (4-methoxyphenyl)(3,4,5-trimethoxyphenyl)methanone. Cancer Chemother. Pharmacol. 68, 45–52.

Magalhães, H.I., Cavalcanti, B.C., Bezerra, D.P., Wilke, D.V., Paiva, J.C.G., Rotta, R., Lima, D.P., Beatriz, A., Burbano, R.R., Costa-Lotufo, L.V., Moraes, M.O., Pessoa, C., 2011b. Assessment of genotoxic effects of (4-methoxyphenyl)(3,4,5-trimethoxyphenyl) methanone in human lymphocytes. Toxicol. *In Vitro* 25, 2048–2053.

Mollinedo, F., Gajate, C., 2003. Microtubules, microtubule-interfering agents and apoptosis. Apoptosis 8, 413–450.
Morris, G.M., Goodsell, D.S., Halliday, R.S., Huey, R., Hart, W.E., Belew, R.K., Olson, A.J., 1998. Automated docking using a Lamarckian genetic algorithm and empirical binding free energy function. J. Comput. Chem. 19, 1639–1662.
Mosmann, T., 1983. Rapid colorimetric assay for cellular growth and survival: application to proliferation and cytotoxicity assays. J. Immunol. Methods 16, 55–63.
Nabha, S.M., Wall, N.R., Mohammad, R.M., Pettit, G.R., Al-Katib, A.M., 2000. Effects of combretastatin A-4 prodrug against a panel of malignant human B-lymphoid cell lines. Anticancer Drugs 11, 385–392.
Nabha, S.M., Mohammad, R.M., Dandashi, M.H., Coupaye-Gerard, B., Aboukameel, A., Pettit, G.R., Al-Katib, A.M., 2002. Combretastatin-A4 prodrug induces mitotic catastrophe in chronic lymphocytic leukemia cell line independent of caspase activation and poly(ADP-ribose) polymerase cleavage. Clin. Cancer Res. 8, 2735–2741.
Nguyen, T.L., McGrath, C., Hermone, A.R., Burnett, J.C., Zaharevitz, D.W., Day, B.W., Wipf, P., Hamel, E., Gussio, R., 2005. A common pharmacophore for a diverse set of colchicine site inhibitors using a structure-based approach. J. Med. Chem. 48, 6107–6116.
Nicoletti, I., Magliorati, G., Pagliacci, M.C., Grignani, F., Riccardi, C., 1991. A rapid and simple method for measuring thymocyte apoptosis by propidium iodide staining and flow cytometry. J. Immunol. Methods 139, 271–279.
Ola, M.S., Nawaz, M., Ahsan, H., 2011. Role of Bcl-2 family proteins and caspases in the regulation of apoptosis. Mol. Cell. Biochem. 351, 41–58.
Pessoa, C., Silveira, E.R., Lemos, T.L., Wetmore, L.A., Moraes, M.O., Leyva, A., 2000. Antiproliferative effects of compounds derived from plants of Northeast Brazil. Phytother. Res. 14, 187–191.
Petit, I., Karajannis, M.A., Vincent, L., Young, L., Butler, J., Hooper, A.T., Shido, K., Steller, H., Chaplin, D.J., Feldman, E., Rafii, S., 2008. The microtubule-targeting agent CA4P regresses leukemic xenografts by disrupting interaction with vascular cells and mitochondrial-dependent cell death. Blood 111, 1951–1961.
Pettit, G.R., Toki, B., Herald, D.L., Verdier-Pinard, P., Boyd, M.R., Hamel, E., Pettit, R.K., 1998. Antineoplastic agents. 379. Synthesis of phenstatin phosphate. J. Med. Chem. 41, 1688–1695.
Prinz, H., Ishii, Y., Hirano, T., Stoiber, T., Camacho Gomez, J.A., Schmidt, P., Düssmann, H., Burger, A.M., Prehn, J.H., Günther, E.G., Unger, E., Umezawa, K., 2003. Novel benzylidene-9(10H)-anthracenones as highly active antimicrotubule agents. Synthesis, antiproliferative activity, and inhibition of tubulin polymerization. J. Med. Chem. 46, 3382–3394.
Prinz, H., Chamasmani, B., Vogel, K., Böhm, K.J., Aicher, B., Gerlach, M., Günther, E.G., Amon, P., Ivanov, I., Müller, K., 2011. N-benzoylated phenoxazines and phenothiazines: synthesis, antiproliferative activity, and inhibition of tubulin polymerization. J. Med. Chem. 54, 4247–4263.
Rappl, C., Barbier, P., Bourgarel-Rey, V., Grégoire, C., Gilli, R., Carre, M., Combes, S., Finet, J.P., Peyrot, V., 2006. Interaction of 4-arylcoumarin analogues of combretastatins with microtubule network of HBL100 cells and binding to tubulin. Biochemistry 45, 9210–9218.
Ravelli, R.B.G., Gigant, B., Curmi, P.A., Jourdain, I., Lachkar, S., Sobel, A., Knossow, M., 2004. Insight into tubulin regulation from a complex with colchicine and a stathmin-like domain. Nature 428, 198–202.
Rycker, M., Rigoreau, L., Dowding, S., Parker, P.J., 2009. A high-content, cell-based screen identifies micropolyin, a new inhibitor of microtubule dynamics. Chem. Biol. Drug Des. 73, 599–610.
Saelens, X., Festjens, N., Vande Walle, L., van Gurp, M., van Loo, G., Vandenabeele, P., 2004. Toxic proteins released from mitochondria in cell death. Oncogene 23, 2861–2874.
Sanner, M.F., Duncan, B.S., Carrillo, C.J., Olson, A.J., 1999. Integrating computation and visualization for biomolecular analysis: an example using python and AVS. Pac. Symp. Biocomput. 401–412.
Schneider, Y., Chabert, P., Stutzmann, J., Coelho, D., Fougerousse, A., Gossé, F., Launay, J.F., Brouillard, R., Raul, F., 2003. Resveratrol analog (*Z*)-3,5,40-trimethoxystilbene is a potent anti-mitotic drug inhibiting tubulin polymerization. Int. J. Cancer 107, 189–196.
Singh, N.P., Mccoy, M.T., Tice, R.R., Schneider, E.L.A., 1988. Single technique for quantitation of low levels of DNA damage in individual cells. Exp. Cell Res. 175, 184–191.
Speit, G., Hartmann, A., 1999. The comet assay (single-cell gel test). A sensitive genotoxicity test for the detection of DNA damage and repair. Methods Mol. Biol. 113, 203–212.
Sureda, F.X., Escubedo, E., Gabriel, C., Comas, J., Camarasa, J., Camins, A., 1997. Mitochondrial membrane potential measurement in rat cerebellar neurons by flow cytometry. Cytometry 28, 74–80.
Vermes, I., Haanen, C., Steffens-Nakken, H., Reutelingsperger, C., 1995. A novel assay for apoptosis. Flow cytometric detection of phosphatidylserine expression on early apoptotic cells using fluorescein labelled Annexin V. J. Immunol. Methods 184, 39–51.
Zhang, D.W., Zhang, J.Z.H., 2003. Molecular fractionation with conjugate caps for full quantum mechanical calculation of protein molecule interaction energy. J. Chem. Phys. 119, 3599–3605.